Available online at www.sciencedirect.com
SCIENCE DIRECT
Journal of Power Sources 152 (2005) 50–59
JOURNAL OF POWER SOURCES
www.elsevier.com/locate/jpowsour

The influence of the nature of the metal on the performance of cerium oxide supported catalysts in the partial oxidation of ethanol☆

L.V. Mattos, F.B. Noronha *

Instituto Nacional de Tecnologia-INT, Av. Venezuela 82, CEP 20081-312 Rio de Janeiro, Brazil

Received 30 November 2004; accepted 26 December 2004
Available online 3 March 2005

Abstract

This work studied the effect of the nature of the metal on the performance of Co/CeO_2, Pd/CeO_2 and Pt/CeO_2 catalysts in the partial oxidation of ethanol. Infrared spectroscopy of adsorbed ethanol and temperature programmed desorption of ethanol were performed in order to establish the reaction mechanism. Catalytic experiments revealed that the product distribution is strongly affected by the nature of the metal. Acetaldehyde was practically the only product formed on a Co/CeO_2 catalyst while methane was also produced on Pt/CeO_2 and Pd/CeO_2 catalysts. These results were explained through a reaction mechanism proposed by the characterization techniques.

Co/CeO_2 and Pt/CeO_2 catalysts show mainly ethoxy species at room temperature whereas acetate species is mainly formed on the Pd/CeO_2 catalyst. The ethoxy species can undergo further dehydrogenation and desorb as acetaldehyde. This effect is more significant with the Co/CeO_2 catalyst and could explain the higher selectivity to acetaldehyde observed on supported Co and Pt catalysts.

Keywords: Fuel cell; Partial oxidation of ethanol; Hydrogen production; Co/CeO_2 catalyst; Pd/CeO_2 catalyst; Pt/CeO_2 catalyst

1. Introduction

The main energy carrier used today is based on carbon fuels. However, burning of hydrocarbon fuels increases the emissions of greenhouse gases, such as CO_2, which has produced a sharp climate change. Furthermore, the economic growth of America and China and instability on the Middle East region has caused a steep rise in oil prices. Clean forms of energy are needed to support global economic growth while reducing the impact on air quality and the potential effects of greenhouse emissions.

Recently, hydrogen has been proposed as a major energy source that could contribute to the reduction of global dependence on fossil fuels, greenhouse gas emissions and atmospheric pollution [1].

Hydrogen can be derived from a variety of energy sources such as biomass, oil, coal and natural gas [2]. It has many applications, including fuel for automobiles and distributed and central electricity and thermal generation. But, the existing hydrogen production and distribution infrastructure is insufficient to support widespread use of hydrogen for energy production [3]. The current hydrogen industry does not produce hydrogen as an energy carrier or as a fuel for energy generation. Therefore, to make a successful transition to the so-called "hydrogen economy", significant technical challenges must be addressed. The most important challenges involve: (i) production, delivery and storage of hydrogen; (ii) end-use energy applications and (iii) conversion of hydrogen to useful energy through fuel cells.

Hydrogen-powered fuel cells represent a radically different approach to energy conversion. These systems directly convert chemical energy into electric power, without the intermediate production of mechanical work [4].

Hydrogen production for fuel cells from local fuel reforming is an alternative to solve the problem of transport

☆ This paper was presented at the 2004 Fuel Cell Seminar, San Antonio, TX, USA.

* Corresponding author. Fax: +55 21 2206 1051.
E-mail address: fabiobel@int.gov.br (F.B. Noronha).

0378-7753/$ – see front matter © 2005 Elsevier B.V. All rights reserved.
doi:10.1016/j.jpowsour.2004.12.052

and storage of hydrogen. Several technologies can be used to produce hydrogen from fuels such as steam reforming (SR), partial oxidation (POX) and autothermal reforming (ATR) [5]. The choice of fuel and fuel processing technology depend on both the type of fuel cell and its application.

Methanol and gasoline are the preferred fuels for automotive applications [6]. While lower temperatures are necessary to produce hydrogen from methanol, gasoline has an established infrastructure. On the other hand, natural gas is considered a promising fuel for stationary power [5]. The disadvantage of the use of this fuel is related to infrastructure, which does not extend to all areas.

Biomass-derived materials are an interesting alternative for hydrogen production since they do not contribute to CO_2 emissions and provide a high energy density and ease of handling. They can be used for hydrogen production for automotive and distributed power generation. Among the compounds available from renewable sources, ethanol is very attractive. Ethanol used in fuel cell vehicles or for stationary power plants generates far fewer greenhouse gases than conventional fuels such as gasoline or natural gas and it is less toxic [7]. Furthermore, the infrastructure needed for ethanol production and distribution is already established in countries like Brazil and USA, since ethanol is currently distributed and used as an octane enhancer or oxygenate blended with gasoline. According to automobile manufacturers, fuel infrastructure is one of the most critical issues in determining the choice of fuel for fuel cell powered vehicles [7]. Ethanol may also play an important role in distributed generation as a fuel source that is available in remote areas where natural gas infrastructure is not present.

Steam reforming of ethanol has been proposed for the production of hydrogen for fuel cells [8–20]. However, this process presents some disadvantages such as formation of byproducts and catalyst deactivation.

The nature of the metal plays an important role in product distribution and on catalyst activity and deactivation in the steam reforming of ethanol. Supported Cu catalysts exhibit a significant formation of by-products such as acid acetic, acetaldehyde and C_4 species on steam reforming of ethanol [8]. Supported Ni and Co catalysts also produce a high production of byproducts (CO, CH_4 and acetaldehyde) on steam reforming of ethanol [21]. The effect of the acid acetic and acetaldehyde on fuel cell efficiency has not been studied yet. Regarding the presence of methane, this compound does not cause damage to the fuel cell systems and it can be used as a fuel for a reformer [22].

Breen et al. [17] studied the behavior of alumina and ceria/zirconia-supported Rh, Pd and Pt catalysts on the steam reforming of ethanol at different temperatures. On alumina supports, the order of activity of the metals was Rh > Pd > Pt. On the other hand, on ceria/zirconia supports, the catalytic activity follows the order Pt ≥ Rh > Pd. For all alumina-supported catalysts, ethene is the main product at low temperatures and this is converted to H_2, CO and CO_2 as the temperature is increased. The production of methane is very low on all catalysts. On the other hand, for ceria/zirconia-supported catalysts, all catalysts did not produce ethene and the main products obtained were H_2, CO, CO_2 and CH_4 even at lower temperatures.

The deactivation of the catalysts is also a problem in the steam reforming of ethanol [15]. Cavallaro et al. [15] compared the performance of supported Co and Rh catalysts on steam reforming of ethanol. Regarding Co catalysts, the decrease of H_2 yield was followed by an increase of acetaldehyde production and a reduction of selectivity toward methane, CO_2 and CO. The deactivation was attributed to coke deposition.

Hence, the economical viability for the use of ethanol as a source of hydrogen for fuel cells depends on the development of new catalysts and the determination of the appropriate reaction conditions.

In spite of the large number of studies on hydrogen production from the steam reforming of ethanol, there are few reports dealing with the use of supported metallic catalysts on the partial oxidation of ethanol [23–25]. Partial oxidation is very interesting, since it has a fast start up and response time, which makes it attractive for rapidly following varying loads. Moreover, the POX reactor is more compact than a steam reformer, since it does not need the indirect addition of heat via a heat exchanger.

Recently, we have investigated the performance of Pt/CeO_2 catalysts on partial oxidation of ethanol [23]. The product distribution strongly depended on the reaction conditions. Increasing both the reaction temperature and the residence time decreased the selectivity to acetaldehyde. The Pt/CeO_2 catalyst was quite stable for partial oxidation of ethanol. The high stability of this catalyst was due to the redox properties of cerium oxide.

In this work, the aim is to study the effect of the metal nature on the performance of Co/CeO_2, Pd/CeO_2 and Pt/CeO_2 catalysts on partial oxidation of ethanol. A reaction mechanism was proposed in order to explain the selectivities observed.

2. Experimental

2.1. Catalyst preparation

The CeO_2 support was prepared by calcination of cerium(IV) ammonium nitrate (Aldrich) at 1073 K for 1 h in a muffle furnace. Platinum (1.5 wt.%), palladium (1.0 wt.%) and cobalt (1.0 wt.%) were added to CeO_2 by incipient wetness impregnation with an aqueous solution containing $H_2PtCl_6{\cdot}6H_2O$, $Pd(NO_3)_2$ and $Co(NO_3)_2$, respectively. After impregnation, the samples were dried at 393 K and calcined under air (50 $cm^3\,min^{-1}$) at 673 K, for 2 h. Then, three catalysts were obtained: Pt/CeO_2, Pd/CeO_2 and Co/CeO_2.

2.2. Infrared spectroscopy of adsorbed ethanol (IR)

Infrared spectroscopy analyses of adsorbed ethanol were performed using a Fourier transform infrared spectrometer (Nicolet, Magna 560). Before the analysis, the samples were reduced with H_2 at 773 K, for 1 h. Then, the samples were evacuated at the reduction temperature for 1 h and cooled down to room temperature. The catalysts were then exposed to 2 Torr of ethanol for 1 h, at room temperature and the spectra were collected after vacuum treatment at 298, 373, 423, 473, 573 and 673 K.

2.3. Temperature programmed desorption of ethanol (TPD)

The temperature programmed desorption experiments of adsorbed ethanol were carried out in a micro-reactor coupled to a quadrupole mass spectrometer (Omnistar, Balzers). Prior to TPD analyses, the samples were reduced under flowing H_2 (30 $cm^3\,min^{-1}$) up to 773 K (5 K min^{-1}), maintaining that temperature for 1 h. Then, the system was purged with helium at 773 K for 30 min and cooled to room temperature. The adsorption of ethanol was made at room temperature through pulses of an ethanol/He mixture, which was obtained by flowing He through a saturator containing ethanol at 298 K. After adsorption, the catalyst was heated at a 20 K min^{-1} rate up to 823 K in flowing helium (50 $cm^3\,min^{-1}$). The products were monitored using a quadrupole mass spectrometer (Balzers, PRISMA). A Quadstar analytical system was used for recording the different signals of masses as a function of the temperature.

2.4. Reaction conditions

Ethanol partial oxidation was performed in a fixed-bed reactor at atmospheric pressure. Prior to reaction, the catalysts were reduced at 773 K, for 1 h, and then purged under N_2 at the same temperature for 30 min. The reaction was carried out at 573 K and $W/F = 0.16\ g\,s\,cm^{-3}$ (for all catalysts) and $0.04\ g\,s\,cm^{-3}$ (for Pt/CeO_2 catalyst). This reaction temperature was chosen due to the negligible ethanol conversion in the absence of catalyst under these conditions [23]. The reactants were fed to the reactor by bubbling air (30 $cm^3\,min^{-1}$) and N_2 (30 $cm^3\,min^{-1}$) through two saturators containing ethanol at 319 K, in order to obtain the desired ethanol/O_2 ratio (2:1). Although the value of ethanol/O_2 ratio of 0.67 is theoretically the best for hydrogen production, Cavallaro et al. [26] showed that ethanol conversion is around 100% and H_2 production reaches a maximum when using an ethanol/O_2 ratio between 1.7 and 2.5 on Rh/Al_2O_3 catalysts. The exit gases were analyzed using two gas chromatographs equipped with a flame ionization and a thermal conductivity detectors, respectively.

Selectivity to hydrocarbons and oxygenated products (selectivity to HC) values reported for each run were evaluated at the same conversion (Pd/CeO_2 and Co/CeO_2: $W/F = 0.16\ g\,s\,cm^{-3}$; Pt/CeO_2: $W/F = 0.04\ g\,s\,cm^{-3}$). The selectivity to HC (S_x) was calculated from

$$S_x = \frac{y_x}{y_M + y_{C_2} + y_{MOH} + y_{acetal} + y_{acetate}} \times 100 \quad (1)$$

where y_x is the weight fraction of the methane ($x = M$), ethane + ethene ($x = C_2$), methanol ($x = MOH$), acetaldehyde ($x = acetal$) or ethyl acetate ($x = acetate$).

3. Results and discussion

3.1. Partial oxidation of ethanol

Fig. 1 shows the ethanol conversion obtained for all catalysts as a function of time on stream (TOS) on partial oxidation of ethanol. Pt/CeO_2 and Co/CeO_2 catalysts produced the higher and the lower values of initial activity, respectively. A deactivation was observed for all samples in the beginning of the reaction, but the catalysts became stable after about 200 min TOS. This deactivation was stronger on the Pd/CeO_2 catalyst.

All catalysts produced a low formation of H_2, CO and CO_2 (not shown). Furthermore, the CO production obtained for Co/CeO_2 catalyst was much lower than that observed for Pd/CeO_2 and Pt/CeO_2 catalysts. Concerning the selectivity to hydrocarbons and oxygenated products (Fig. 2), acetaldehyde was practically the only product formed on Co/CeO_2 catalyst. On the other hand, acetaldehyde as well as methane were observed on Pd/CeO_2 and Pt/CeO_2 catalysts. However, the acetaldehyde production was lower on the Pd/CeO_2 catalyst. Only trace amounts of C2 were detected for all samples. Moreover, a small quantity of ethyl acetate was observed on the Pd/CeO_2 catalyst. The nature of the metal strongly affected the selectivity to products. In order to explain the selectivities observed, a reaction mechanism was proposed, using infrared spectroscopy analyses of adsorbed ethanol, temperature programmed desorption of ethanol and temperature programmed surface reaction.

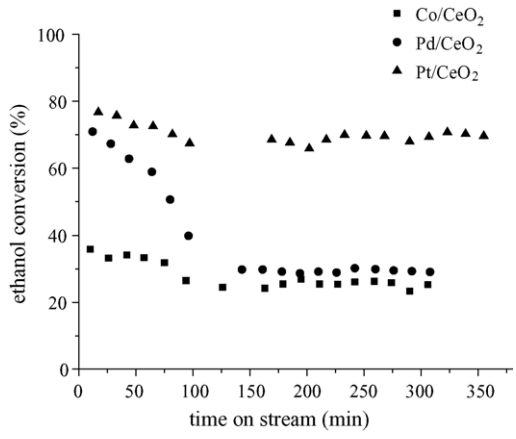

Fig. 1. Ethanol conversion obtained for all catalysts as a function of time on stream (TOS) on partial oxidation of ethanol ($T_{reaction} = 573$ K and $W/F = 0.16\ g\,s\,cm^{-3}$).

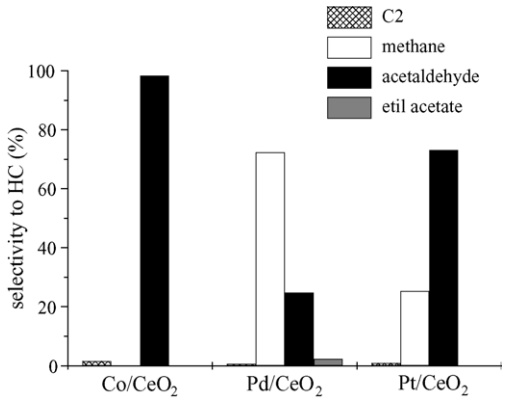

Fig. 2. Selectivity to hydrocarbons and oxygenated products (selectivity to HC) obtained for all catalysts on partial oxidation of ethanol at the same conversion (around 40%). Reaction conditions: $T_{reaction}$ = 573 K; W/F = 0.16 g s cm^{-3} (for Co/CeO$_2$ and Pd/CeO$_2$ catalysts) and 0.04 g s cm^{-3} (for Pt/CeO$_2$ catalyst).

3.2. Infrared spectroscopy of adsorbed ethanol

Figs. 3 and 4 show the IR spectra of adsorbed ethanol at different temperatures between 1800 and 1000 and 3000 and 2500 cm^{-1}, respectively, on Co/CeO$_2$, Pd/CeO$_2$ and Pt/CeO$_2$ catalysts. For the Co/CeO$_2$ catalyst, the IR spectrum after ethanol adsorption and evacuation at room temperature exhibited bands at 1049, 1100, 1115, 1383, 1429, 1552, 2862, 2928 and 2962 cm^{-1}. For the Pd/CeO$_2$ catalyst, the IR spectrum presented bands at 1018, 1049, 1092, 1116, 1340, 1439, 1545, 2868, 2931 and 2964 cm^{-1}. On the Pt/CeO$_2$ catalyst, we observed bands at 1040, 1082, 1315, 1340, 1400, 1425, 1525, 1574, 1600, 1687, 2933 and 2978 cm^{-1}. In the literature, alcohols such as ethanol [27–29] and methanol [30–33] adsorb on the surface of metal oxides through an alkoxide species formed from the scission of the O–H bond. The bands at 1040, 1082, 1092, 1100, 1115, 1116 and 1383, 1400, 2868, 2862, 2928, 2931, 2933, 2962, 2964 and 2978 cm^{-1} can be attributed to ethoxy species [27–29]. The bands at 1018, 1049, 1302, 1315, 1340, 1425, 1429,

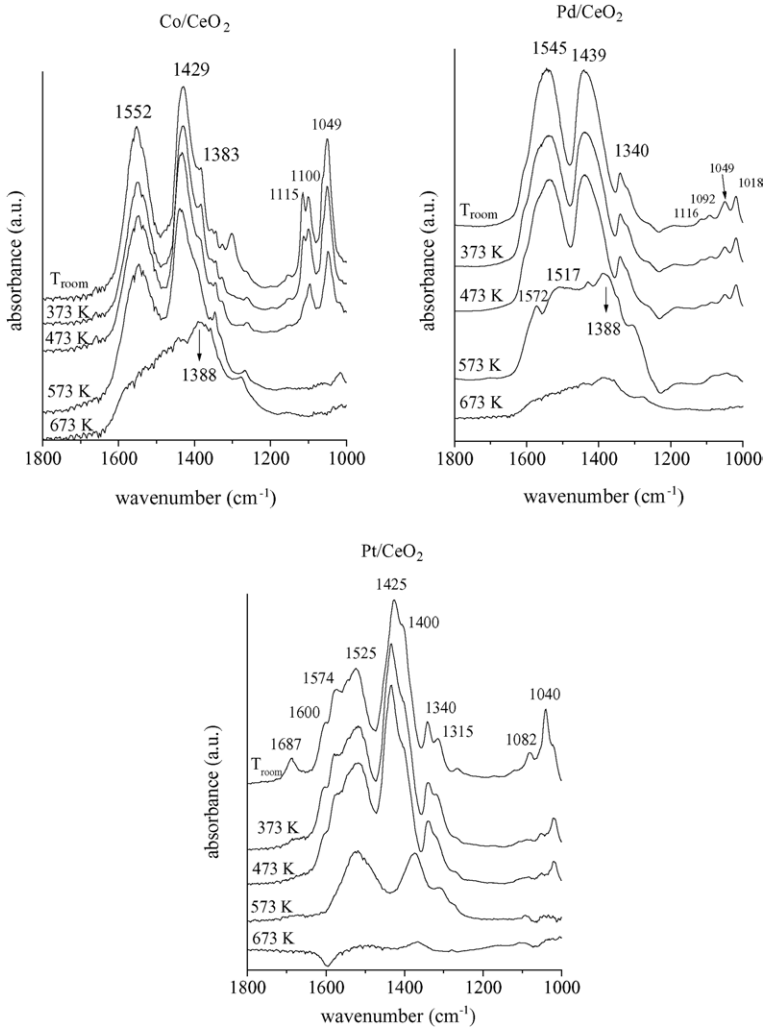

Fig. 3. Infrared spectra of the surface species formed by ethanol adsorption between 1800 and 1000 cm^{-1} on reduced Co/CeO$_2$, Pd/CeO$_2$ and Pt/CeO$_2$ catalysts at different temperatures.

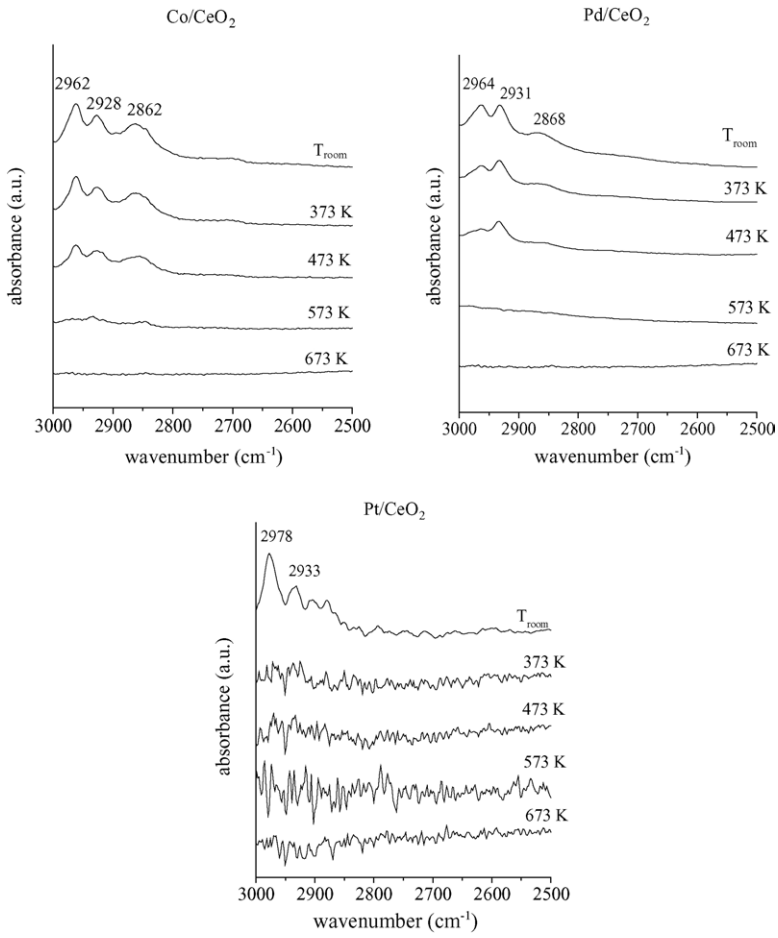

Fig. 4. Infrared spectra of the surface species formed by ethanol adsorption between 3000 and 2500 cm^{-1} on reduced Co/CeO_2, Pd/CeO_2 and Pt/CeO_2 catalysts at different temperatures.

1439, 1545, 1552, 1564, 1574 and 1600 cm^{-1} can be assigned to acetate species, which were produced by oxidation of ethoxy species [28,29]. The formation of ethoxy species decreased in the order $Co/CeO_2 \gg Pt/CeO_2 > Pd/CeO_2$, while the acetate species production follows the opposite trend ($Pd/CeO_2 \gg Pt/CeO_2 > Co/CeO_2$).

Idriss and co workers [28,29,34] suggest that the ethanol adsorbs dissociatively to form ethoxy species on CeO_2 [28], Pd/CeO_2 [28], Pt/CeO_2 [29] and Rh/CeO_2 [34] at room temperature, using IR spectroscopy. At this temperature, acetate species were only observed on unreduced CeO_2. According to these authors, the absence of acetate species on reduced CeO_2 and supported catalysts (unreduced and reduced) was due to partial reduction of support.

In this work, the presence of acetate species on supported CeO_2 catalysts at room temperature could be attributed to the redox properties of ceria. Several studies reported that cerium oxide has a very high oxygen exchange capacity [35,36]. This capacity is associated with the ability of cerium to act as an oxygen buffer by storing/releasing O_2 due to the Ce^{4+}/Ce^{3+} redox couple [36]. The OSC measurement of our Pt/CeO_2 catalyst corresponds to around 13% of Ce^{3+} on the support [23]. Deeper reduction of CeO_2 samples have been reported after treatment at higher temperatures [37,38]. This means that a large amount of mobile oxygen is still available after reduction at 773 K. Unfortunately, Idriss and co workers [28,29,34] measured neither the oxygen storage capacity of their catalysts nor the extent of support reduction. So, a comparison between both works is difficult to be established. The redox properties of their materials could possibly explain the differences observed. Nevertheless, it seems that their Pd/CeO_2, Pt/CeO_2 and Rh/CeO_2 catalysts have a lower capacity to exchange oxygen than the catalysts studied in this work.

Moreover, Finacchio et al. [31] proposed that the oxidation of ethoxy to acetate species occurs in parallel to the $Ce^{4+} \rightarrow Ce^{3+}$ reduction. According to the authors, the adsorption of methanol on Ce^{4+} sites led to the production of formate species ($HCOO^-$) and H_2, which was accompanied by $Ce^{4+} \rightarrow Ce^{3+}$ reduction.

At 373 K, the bands corresponding to ethoxy and acetate species did not undergo significant changes on Co/CeO_2 and Pd/CeO_2 catalysts. However, on the Pt/CeO_2 catalyst, the bands corresponding to ethoxy species almost completely disappeared at 373 K, while the intensity of the bands associated with acetate species remained unchanged. After heating

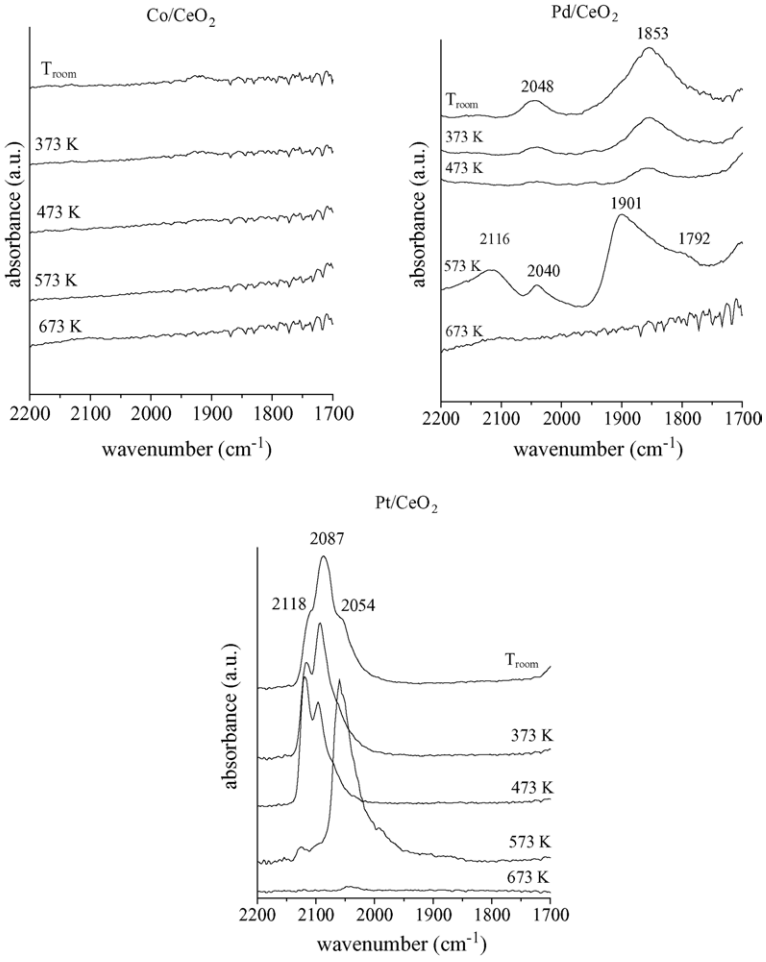

Fig. 5. Infrared spectra of the surface species formed by ethanol adsorption between 2200 and 1700 cm^{-1} on reduced Co/CeO_2, Pd/CeO_2 and Pt/CeO_2 catalysts at different temperatures.

Co/CeO_2 and Pd/CeO_2 catalysts at 473 K, the intensity of the bands corresponding to ethoxy species was reduced, whereas the bands associated with acetate species remained practically unchanged. For the Pt/CeO_2 catalyst, in the IR spectrum, significant changes were not seen when the sample was heated to 473 K. Therefore, the reduction of intensity of the bands of ethoxy species was not followed by the formation of acetate species on all catalysts. When the Co/CeO_2 catalyst was heated to 573 K, the bands related to the ethoxy species were no longer detected, while the bands characteristic of the acetate species were still present. For the Pd/CeO_2 and Pt/CeO_2 catalysts, heating to 573 K resulted in important changes on the spectra. All the bands attributed to acetate and ethoxy species were no longer detected. However, the bands characteristic of carbonate species (1572, 1523, 1517, 1388 and 1375 cm^{-1}) were now present. This result indicates that the Pd/CeO_2 and Pt/CeO_2 catalysts were more reactive than the Co/CeO_2 catalyst. Only at high temperature (673 K), the IR spectra obtained on Co/CeO_2 catalyst exhibited the band for carbonate species (1388 cm^{-1}) and no bands associated with acetate species were observed. For the Pd/CeO_2 and Pt/CeO_2 catalysts, the intensity of the bands related to carbonate species were strongly reduced at 673 K.

The bands observed between 2200 and 1700 cm^{-1} have been attributed to CO adsorption on metal particles (Fig. 5) [39–44]. These bands can be divided into two regions. The first region corresponds to the absorption bands between 2200 and 1900 cm^{-1}, which have been assigned to linearly adsorbed CO. The second region corresponds to the bands between 1900 and 1700 cm^{-1}, which are due to bridged or multi-coordinated adsorbed CO [45–47].

In this work, the Co/CeO_2 catalyst did not produce bands corresponding to CO adsorption (Fig. 5) at all the temperatures studied. This result agrees with that obtained by partial oxidation of ethanol. As previously described, the Co/CeO_2 catalyst showed a lower production of CO during this reaction. At room temperature, the Pd/CeO_2 catalyst showed bands at 2048 and 1853 cm^{-1}. Moreover, the intensity of the band at 1853 cm^{-1} was stronger than that obtained for the band at 2048 cm^{-1}. The Pt/CeO_2 catalyst produce bands at 2118, 2087 and 2054 cm^{-1}. The bands at 2087, 2054 and 2048 cm^{-1} can be attributed to linearly adsorbed CO on Pd

and Pt particles with different sizes. The band at 1853 cm^{-1} can be assigned to multi-coordinated adsorbed CO on Pd particles. These results showed that Pd had mainly bridged or multi-coordinated adsorbed CO, which is in agreement with the literature [43,44].

The band at 2118 cm^{-1} has been related to the CO adsorption on Pt^{2+} [41] and on Pd^{2+} [48]. However, this band has also been observed in the IR spectra in the absence of noble metal. Yee et al. [29] detected a band at 2122 cm^{-1} in the IR spectra of reduced CeO_2 samples (before ethanol adsorption), which was formed by carbonate decomposition during reduction. They attributed this band to CO adsorbed on Ce^{3+} cations. Furthermore, this band only appeared on the unreduced and reduced Pt/CeO_2 catalyst after ethanol adsorption and heating at 523 K. The appearance of this band was followed by the formation of carbonate species. Therefore, in our work, the band at 2118 cm^{-1} could possibly be assigned to the CO adsorption on Ce^{3+} cations, as previously reported [29].

Increasing the temperature to 473 K strongly decreased the absorbance of the bands of CO linearly adsorbed on Pd and Pt whereas the band at 2118 cm^{-1} was practically unaffected. When the temperature was increased to 573 K, the appearance of bands at 2116, 2040, 1901 and 1792 cm^{-1} on Pd/CeO_2 catalyst was observed. On the other hand, for the Pt/CeO_2 catalyst, the band at 2118 cm^{-1} disappeared and the intensity of the band at 2054 cm^{-1} increased at 573 K.

Eischens et al. [49] and Bradshaw and Hoffmann [50] studied the CO adsorption on a Pd catalyst under different surface coverages. The CO frequency on the Pd surface varies from 1834 cm^{-1} at low coverages to 1924 cm^{-1} at high coverages [49]. The shift as a function of coverage was explained in terms of adsorption on a multiplicity of crystal planes [50]. Bradshaw and Hoffmann [50] proposed that two-fold co-ordination sites give rise to a band in the range of 1880–2000 cm^{-1} at $\theta > 0.4$. At low surface coverage ($\theta < 0.4$), a band in the region 1800–1880 cm^{-1} was attributed to three-fold co-ordination sites.

Therefore, in our work, the shift of the CO frequency from 1853 to 1901 cm^{-1} corresponds to the increase of Pd surface coverage as the temperature increases.

It is important to stress that the presence of CO adsorbed at room temperature on Pd/CeO_2 and Pt/CeO_2 catalysts stems from the ethoxy species decomposition, in agreement with the TPD analysis, which will be presented next.

3.3. Temperature programmed desorption of ethanol

The TPD profiles of adsorbed ethanol on Co/CeO_2 and Pt/CeO_2 catalysts are shown in Fig. 6. Ethanol desorbed at 520 and 422 K on Co/CeO_2 and Pt/CeO_2 catalysts, respectively. Furthermore, no acetaldehyde formation was detected on both catalysts. The same result was obtained by Yee et al. [28] while studying the adsorption of ethanol on unreduced CeO_2. According to them, dehydrogenation of ethoxy species to acetaldehyde is followed by a very facile oxidation to acetate species due to the high amount of oxygen available. This could explain the absence of acetaldehyde species on CeO_2 surface and agrees very well with the redox properties of our catalyst.

Co/CeO_2 catalyst exhibited the formation of CO, CH_4 and H_2 at around 600 K. For Pt/CeO_2 catalysts, the production of CO, CH_4 and H_2 began at lower temperatures (around 350 K). According to IR analysis, the ethoxy species completely disappeared at 573 K and 373 K, on Co/CeO_2 and Pt/CeO_2 catalysts, respectively. Taking into account the results obtained by TPD and IR experiments, the formation of CO, CH_4 and H_2 could be attributed to the decomposition of adsorbed ethoxy species, which occurred at higher temperatures on Co/CeO_2 catalyst. Several authors have reported the appearance of CO, CH_4 and H_2 in the low temperature region during TPD analysis of adsorbed ethanol, which was attributed to the decomposition of ethoxy species [28,51–53]. Cordi and Falconer [52] suggested that part of the ethanol adsorbed on alumina forms ethoxy species that migrates to Pd sites where decomposition take places. According to them,

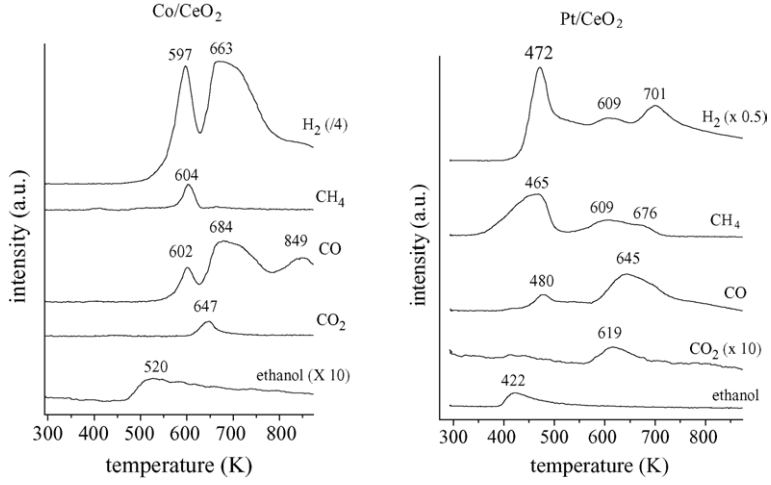

Fig. 6. TPD profile of ethanol adsorbed on Co/CeO_2 and Pt/CeO_2 catalysts.

the α-carbon produced CO and the β-carbon formed CH_4 during ethanol decomposition. CO, CH_4 and H_2 were also produced at 495 K during TPD experiment of ethanol on Pd/Al_2O_3 catalyst, due to the decomposition of ethanol on Pd [51].

The TPD analysis also showed a further formation of CO, H_2 and the appearance of CO_2 at higher temperatures for the Co/CeO_2 catalyst (above 630 K) and the Pt/CeO_2 catalyst (above 550 K). For the Pt/CeO_2 catalyst, methane was also produced above 550 K. As observed in the IR experiments, the bands related to acetate species vanished and the bands corresponding to carbonate species were detected at 673 and 573 K, on Co/CeO_2 and Pt/CeO_2 catalysts, respectively. These results suggest that the acetate species underwent further oxidation, producing carbonate species, as well as decomposition to CO and CH_4. The formation of carbonate species and the decomposition of acetate species were observed at higher temperature on the Co/CeO_2 catalyst.

CO_2 formation can be assigned to decomposition of carbonate species on both samples. However, the amount of CO_2 formed is low, which could be attributed to CO_2 dissociation on oxygen vacancies of the support, producing CO. We have previously reported that CO_2 can replenish the oxygen vacancies of the support, releasing CO as a product [54,55]. This agrees very well with the CO evolution detected at high temperature on our TPD analysis. The production of CO, CO_2 and H_2 at high temperatures on alumina supported catalyts has also been reported [51,52]. According to Cordi and Falconer [52], it might be due to the decomposition of a more stable carbon species formed during ethanol decomposition at lower temperatures. They further suggested that acetaldehyde or acetic acid could be the precursor for this more stable carbon species. Baldanza et al. [51] studied the adsorption of ethanol on Pd/Al_2O_3 and $Pd\text{-}Mo/Al_2O_3$ catalysts, using infrared spectroscopy. The results showed the formation of acetate species as the temperature was raised from 523 to 573 K. According to these authors, ethanol is dehydrogenated on Pd sites to form acetaldehyde as well as more stable acetate species. These species remain adsorbed and are the precursors for the CO, H_2 and CO_2 production observed at high temperature. A comparison between ceria and alumina supports showed that acetate species are formed at higher temperatures on alumina due to the lower ability to release/store oxygen of this support. Furthermore, in this case, an important desorption of CO_2 at high temperature is observed because alumina does not have oxygen vacancies as cerium oxide.

Finally, the large H_2 production detected on the TPD profile for Co/CeO_2 and Pt/CeO_2 catalysts at high temperatures could be attributed to the desorption of previously formed hydrogen. We have carried out TPD studies of H_2 adsorbed on this Pt/CeO_2 catalyst [56] and the H_2 signal exhibited two peaks at 353 and 613K. The low temperature peak was assigned to the hydrogen desorption from the metal surface whereas the other one was due to the hydrogen from the support, which was previously transferred from the metal to the support (spill over) [57]. In this work, the hydrogen production peak agrees very well with our previous results.

3.4. Reaction mechanism

In the literature, there are several studies about the reaction mechanism of steam reforming of ethanol [58–61]. However, scarce information is available about the ethanol partial oxidation reaction mechanism. Sheng et al. [24] observed that the increase of reaction temperature from 473 to 673 K led to the decrease of acetaldehyde production and the increase of methane formation on partial oxidation of ethanol over $Rh\text{-}Pt/CeO_2$ catalysts. According to them, ethanol adsorbs as ethoxy species that further reacts to form acetaldehyde. They suggested that acetaldehyde decomposes producing CO and CH_4 at high temperatures, but acetate formation was not proposed.

We have performed temperature programmed surface reaction (TPSR) of ethanol with oxygen on Pt/CeO_2 catalyst in order to study the reaction mechanism [23]. Acetaldehyde was formed at around 426 K with the simultaneous production of CH_4, CO and CO_2. At 545 K, a large production of CO_2 and a small formation of methane occurred. Oxygen consumption was seen at 434 and 548 K.

The comparison of the TPD to TPSR experiments shows that, in the presence of oxygen, not only does the decomposition of ethoxy species take place but also the oxidative dehydrogenation to acetaldehyde. This result suggest that ethoxy species formed on the surface underwent oxidation by the oxygen from the feed simultaneously to its decomposition. This fact could explain the simultaneous observation of acetaldehyde desorption and methane formation. At high temperature, the acetate species formed at room temperature and that remained unreacted are oxidized producing more CO_2.

The participation of acetate species as an intermediate that take part of the reaction mechanism was also suggested by other authors [62]. Nagal and Gonzales [62] studied the oxidation of ethanol and acetaldehyde on Pt/SiO_2 catalysts using in-situ infrared analyses. According to their observations, they proposed a reaction mechanism in which the dehydrogenation of an adsorbed ethoxy species would be the limiting step. These dehydrogenated species could then be oxidized to form intermediate acetate species that would react originating CO_2.

Based on our results obtained by infrared spectroscopy of adsorbed ethanol, temperature programmed desorption of ethanol and temperature programmed surface reaction (TPSR), the following reaction mechanism could be proposed for the partial oxidation of ethanol on Co/CeO_2, Pd/CeO_2 and Pt/CeO_2 catalysts:

At first, ethanol adsorbs on ceria producing an ethoxy species (Eq. (2)). In the absence of oxygen in the feed, a fraction of the ethoxy species can be dehydrogenated and immediately react with oxygen from the support to form acetate species (Eq. (3)), which is followed by the $Ce^{4+} \rightarrow Ce^{3+}$ reduction. Increasing the temperature, another fraction of

the ethoxy species can be decomposed on Pt sites, forming CH_4, H_2 and CO (Eq. (4)). At high temperature, the acetate species previously formed can be decomposed to CH_4 (Eq. (5)) and/or oxidized to CO_2 via carbonate species (Eq. (6)). Under oxygen atmosphere, the intermediate dehydrogenated species formed as indicated above in the first part of Eq. (5) may desorb as acetaldehyde while the Ce^{4+}–O site is recovered (Eq. (7)). This is evidenced by comparing the TPD results, where no acetaldehyde was observed, with the TPSR results, where acetaldehyde formation occurred. The other steps are similar to the ones described in the absence of oxygen in the feed.

$$CH_3CH_2OH(g) + Ce^{4+} \rightarrow CH_3CH_2O{-}Ce^{4+} + \tfrac{1}{2}H_2 \quad (2)$$

$$CH_3CH_2O{-}Ce^{4+} - \tfrac{1}{2}H_2 \rightarrow CH_3CHO{-}Ce^{4+} + Ce^{4+}{-}O^{2-} \rightarrow CH_3COO{-}Ce^{3+} + Ce^{3+} + \tfrac{1}{2}H_2 \quad (3)$$

$$CH_3CH_2O{-}Ce^{4+} \rightarrow CH_4 + CO + \tfrac{1}{2}H_2 + Ce^{4+} \quad (4)$$

$$Ce^{4+}{-}OH + CH_3COO{-}Ce^{3+} \rightarrow CH_4 + {CO_3}^{-}{-}Ce^{4+} + Ce^{3+} \quad (5)$$

$${CO_3}^{-}{-}Ce^{4+} \rightarrow Ce^{4+}{-}O + CO_2 \quad (6)$$

$$CH_3CH_2O{-}Ce^{4+} - \tfrac{1}{2}H_2 \rightarrow CH_3CHO{-}Ce^{4+} + \tfrac{1}{2}O_2(g) \rightarrow CH_3CHO(g) + Ce^{4+}{-}O \quad (7)$$

On the Co/CeO_2 and the Pt/CeO_2 catalysts, IR analysis revealed a higher fraction of ethoxy species at low temperatures than the Pd/CeO_2 catalysts. These ethoxy species can undergo further dehydrogenation and desorb as acetaldehyde as indicate in Eq. (7). This effect is more significant on the Co/CeO_2 catalyst and could explain the higher selectivity to acetaldehyde observed on supported Co and Pt catalyst (Fig. 2).

4. Conclusions

The results obtained showed that the nature of the metal strongly affected the product distribution. The Pt/CeO_2 catalyst showed higher stability on partial oxidation of ethanol. However, in by-product formation, Pd/CeO_2 exhibited the lowest acetaldehyde production. A reaction mechanism was proposed to explain the partial oxidation of ethanol on Co/CeO_2, Pd/CeO_2 and Pt/CeO_2 catalysts based on the IR and TPD experiments. According to this mechanism, adsorption of ethanol on the support gave rise to ethoxy species. The amount of ethoxy species formed followed the order: $Co/CeO_2 \gg Pt/CeO_2 > Pd/CeO_2$. A fraction of this ethoxy species can be dehydrogenated and can further react with oxygen from the support producing acetate species and/or may desorb as acetaldehyde. On the Co/CeO_2 (mainly) and the Pt/CeO_2 catalysts, the dehydrogenated species preferentially desorbs, producing acetaldehyde. On the Pd/CeO_2 catalyst, the dehydrogenated species is further oxidized to acetate species. At high conversions, another fraction of the ethoxy species can be decomposed on the metal sites, forming CH_4, H_2 and CO while the acetate species can be decomposed to CH_4 and/or oxidized to CO_2 via carbonate species.

Acknowledgements

The authors wish to acknowledge the financial support of the CNPq and CNPq/Edital Universal program (476954/01-0).

References

[1] V.A. Goltsov, T.N. Veziroglu, Int. J. Hydrogen Energy 26 (2001) 909.
[2] A.L. Dicks, J. Power Sources 61 (1996) 113.
[3] J. Petrovic, J. Milliken, P. Devlin, C. Read, Proceedings of 2003 Fuel Cell Seminar, Miami Beach, FL, 2003, p. 988.
[4] J. Strakey, M. Williams, Proceedings of 2003 Fuel Cell Seminar, Miami Beach, FL, 2003, p. 756.
[5] J.R. Rostrup-Nielsen, Phys. Chem. Chem. Phys. 3 (2001) 283.
[6] J. Han, I. Kim, K.S. Choi, J. Power Sources 86 (2000) 223.
[7] J. Bentley, R. Derby, Ethanol and Fuel Cells: Converging Paths of Opportunity, report for the Renewable Fuels Association, 2002.
[8] N. Takezawa, N. Iwasa, Catal. Today 36 (1997) 45.
[9] F.J. Marino, E.G. Cerrela, S. Duhalde, M. Jobbagy, M.A. Laborde, Int. J. Hydrogen Energy 12 (1998) 1095.
[10] F.J. Marino, M. Boveri, G. Baronetti, M. Laborde, Int. J. Hydrogen Energy 26 (2001) 665.
[11] E.Y. Garcia, M.A. Laborde, Int. J. Hydrogen Energy 16 (1991) 307.
[12] S. Freni, N. Mondello, S. Cavallaro, G. Cacciola, V.N. Parmon, V.A. Sobyanin, React. Kinet. Catal. Lett. 71 (2000) 143.
[13] V.V. Galvita, G.L. Semin, V.D. Belyaev, V.A. Semikolenov, P. Tsiakaras, V.A. Sobyanin, Appl. Catal. A: Gen. 220 (2001) 123.
[14] A.N. Fatsikostas, D.I. Kondarides, X.E. Verykios, Chem. Commun. 851 (2001).
[15] S. Cavallaro, N. Mondello, S. Freni, J. Power Sources 102 (2001) 198.
[16] A.N. Fatsikostas, D.I. Kondarides, X.E. Verykios, Catal. Today 75 (2002) 145.
[17] J.P. Breen, R. Burch, H.M. Coleman, Appl. Catal. B: Environ. 39 (2002) 65.
[18] J. Llorca, N. Homs, J. Sales, P.R. de la Piscina, J. Catal. 209 (2002) 306.
[19] J. Comas, F. Mariño, M. Laborde, N. Amadeo, Chem. Eng. J. 98 (2004) 61.
[20] M.S. Batista, R.K.S. Santos, E.M. Assaf, J.M. Assaf, E.A. Ticianelli, J. Power Sources 124 (2003) 99.
[21] S. Freni, S. Cavallaro, N. Mondello, M. Minutoli, F. Frusteri, Proceedings of 17th North American Catalysis Society Meeting, Toronto, 2001, p. 135.
[22] T. Ioannides, J. Power Sources 92 (2001) 17.
[23] L.V. Mattos, F.B. Noronha, Appl. Catal. B: Environ., submitted for publication.
[24] P.-Y. Sheng, A. Yee, G.A. Bowmaker, H. Idriss, J. Catal. 208 (2002) 393.

[25] D.K. Liguras, K. Goundani, X.E. Verykios, Int. J. Hydrogen Energy 29 (2004) 419.
[26] S. Cavallaro, V. Chiodo, A. Vita, S. Freni, J. Power Sources 123 (2003) 10.
[27] H. Idriss, C. Diagne, J.P. Hindermann, A. Kiennemann, M.A. Barteau, J. Catal. 155 (1995) 219.
[28] A. Yee, S.J. Morrison, H. Idriss, J. Catal. 186 (1999) 279.
[29] A. Yee, S.J. Morrison, H. Idriss, J. Catal. 191 (2000) 30.
[30] C. Binet, M. Daturi, J.C. Lavalley, Catal. Today 50 (1999) 207.
[31] E. Finocchio, M. Daturi, C. Binet, J.C. Lavalley, G. Blanchard, Catal. Today 52 (1999) 53.
[32] A. Badri, C. Binet, J.C. Lavalley, J. Chem. Soc. Faraday Trans. 93 (1997) 1159.
[33] M. Badlani, I. Wachs, Catal. Lett. 75 (2001) 137.
[34] A. Yee, S.J. Morrison, H. Idriss, Catal. Today 63 (2000) 327.
[35] J. Kaspar, P. Fornasiero, M. Graziani, Catal. Today 50 (1999) 285.
[36] M.H. Yao, R.J. Baird, F.W. Kunz, T.E. Hoost, J. Catal. 166 (1997) 67.
[37] F. Fally, V. Perrichon, H. Vidal, J. Kaspar, G. Blanco, J.M. Pintado, S. Bernal, G. Colon, M. Daturi, J.C. Lavalley, Catal. Today 59 (2000) 373.
[38] H. Vidal, J. Kaspar, M. Pijolat, G. Colon, S. Bernal, A. Cordon, V. Perrichon, F. Fally, Appl. Catal. B: Environ. 27 (2000) 49.
[39] C. Besoukhavnova, J. Guidot, D. Barthomeuf, M. Breysse, J.R. Bernard, J. Chem. Soc. Faraday Trans. 1 77 (1981) 1595.
[40] B.L. Mojet, J.T. Miller, D.C. Koningsberger, J. Phys. Chem. 103 (1999) 2724.
[41] G. Jacobs, F.G. Ghadiali, A. Pisanu, A. Borgna, W.E. Alvarez, D.E. Resasco, Appl. Catal. 188 (1999) 79.
[42] A.Y. Stakheev, E.S. Shpiro, N.I. Jaeger, G. Schulz-Ekloff, Catal. Lett. 32 (1995) 147.
[43] R.F. Hicks, Q. Yen, A.T. Bell, J. Catal. 89 (1984) 498.
[44] M.A. Vannice, S.-Y. Wang, J. Phys. Chem. 85 (1981) 2543.
[45] P.V. Menacherry, G.L. Haller, J. Catal. 177 (1998) 175.
[46] H. Bischoff, N.I. Jaeger, G. Schulz-Ekloff, L. Kubelkova, J. Mol. Catal. 80 (1993) 95.
[47] M. Primet, J. Catal. 88 (1984) 273.
[48] S. Yang, A. Maroto-Valiente, M. Benito-Gonzalez, I. Rodriguez-Ramos, A. Guerrero-Ruiz, Appl. Catal. B 28 (2000) 223.
[49] R.P. Eischens, S.A. Frances, W.A. Pliskin, J. Phys. Chem. 60 (1956) 194.
[50] A.M. Bradshaw, F.M. Hoffmann, Surf. Sci. 72 (1978) 513.
[51] M.A.S. Baldanza, L.F. de Mello, A. Vannice, F.B. Noronha, M. Schmal, J. Catal. 192 (2000) 64.
[52] E.M. Cordi, J.L. Falconer, J. Catal. 162 (1996) 104.
[53] L.F. de Mello, F.B. Noronha, M. Schmal, J. Catal. 220 (2003) 358.
[54] F.B. Noronha, G. Fendley, R.R. Soares, W.E. Alvarez, D.E. Resasco, Chem. Eng. J. 11 (2001) 3775.
[55] S.M. Stagg-Williams, F.B. Noronha, G. Fendley, D.E. Resasco, J. Catal. 194 (2000) 240.
[56] E.R. de Oliveira, L.V. Mattos, F.B. Noronha, F.B. Passos, Proceedings of 11th Brazilian Congress on Catalysis, vol. 1, 2001, p. 529.
[57] S. Bernal, J.J. Calvino, M.A. Cauqui, J.M. Gatica, C. Larese, J.A. Perez Ornil, J.M. Pintado, Catal. Today 50 (1999) 175.
[58] A.N. Fatsikostas, X.E. Verykios, J. Catal. 225 (2004) 439.
[59] C. Diagne, H. Idriss, A. Kiennemann, Catal. Commun. 3 (2002) 565.
[60] V. Klouz, V. Fierro, P. Denton, H. Katz, J.P. Lisse, S. Bouvot-Mauduit, C. Mirodatos, J. Power Sources 105 (2002) 26.
[61] A.N. Fatsikostas, D.I. Kondarides, X.E. Verykios, Catal. Today 75 (2002) 145.
[62] M. Nagal, R.D. Gonzalez, Ind. Eng. Chem. Prod. Res. Dev. 24 (1985) 525.